Acta Montanistica Slovaca
ISSN 1335-1788
actamont.tuke.sk

The effect of the seam slopes on the strata behavior in the longwall coal mines using numerical modeling

***Emad Ansari ARDEHJANI*[1], *Ramin RAFIEE*[2*] and *Mohammad ATAEI*[3]**

Authors' affiliations and addresses:
[1] Faculty of Mining, Petroleum & Geophysics Eng., Shahrood University of Technology, Shahrood, Iran
e-mail: eaa.emad14@gmail.com

[2] Faculty of Mining, Petroleum & Geophysics Eng., Shahrood University of Technology, Shahrood, Iran
e-mail: raminlamezi@gmail.com
e-mail: raminrafiee@shahroodut.ac.ir

[3] Faculty of Mining, Petroleum & Geophysics Eng., Shahrood University of Technology, Shahrood, Iran
e-mail: ataei@shahroodut.ac.ir

***Correspondence:**
Ramin Rafiee, Faculty of Mining, Petroleum & Geophysics Eng., Shahrood University of Technology, Shahrood, Iran
e-mail: raminrafiee@shahroodut.ac.ir

How to cite this article:
Ardehjani, E. A., Rafiee, R. and Ataei M. (2022). The effect of the seam slopes on the strata behavior in the longwall coal mines using numerical modeling. *Acta Montanistica Slovaca,* Volume 27 (1), 27-39

DOI:
https://doi.org/10.46544/AMS.v27i01.03

Abstract
The main factor involved in a successful longwall mining method is proper control and prediction of the roof behavior in the gob area. Thus, the safety and continuity of mining can be guaranteed by recognizing the roof seam behavior and determining the time of roof fall (first fall and periodic fall). Due to the Middle East tectonic conditions, the coal seams in Iran are usually inclined, so studying the seam behavior and face stability in different slopes in underground mining is necessary. In this research, four different block models were simulated to investigate the roof and face behaviors in the 0-, 5-, 10-, and 15-degree slopes using the FLAC3D software. The validation of these models is based on the simulation of the E3 panel of the Tabas Parvade coal mine. Based on the numerical modeling results, the values for the first roof weighting effect interval (FRWEI) in the 0-, 5-, 10-, and 15-degree slopes were calculated to be equal to 26, 29.09, 31.38, and 36 m, respectively. According to these results, the gob roof displacement decreased by increasing the seam slope, and the roof stability time increased. Also, the instability risk of the face and the roof above it was reduced by increasing the seam slope.

Keywords
Longwall mining, Seam slopes, Roof caving, Face stability, Roof weighting effect interval.

Introduction

Upon completion of surface resources, the focus on the extraction and exploitation of underground resources has increased. The underground methods have always challenged the miners due to the complexity of the geological structures and seam behavior during mining. Accordingly, recognizing the layer behavior and geological structures of the seam help to ensure a safe and economical operation of these methods. Longwall mining is a caving underground extraction method that is used widely to extract horizontal coal seams. For the successful operation of the longwall mining, the destructibility of the surrounding rock at the top of the coal seam is essential. In other words, for a proper and safe operation of longwall mining, studying the strata behavior during face advance at longwall mining is important. For this aim, studying the trend of the strata failure and their behavior is essential (Ataei, 2015; Hosseini et al., 2014).

An essential issue in the drilling of underground spaces is the stability of the roof and walls. Due to low coal resistance, coal mines have a high sensitivity from the stability vision. Accordingly, another major issue in the longwall method is the stability of the face based on the gob-induced stresses. Therefore, in the longwall method, assessment of the face stability and the caving behavior of the roof seam in the gob is important.

Recently, many researchers have studied seam's behavior in underground mining. Das proposed a comprehensive classification to investigate the strata failure and the failure type in India (Das, 2000). Oraei and Rostami used a fuzzy method to determine the influence of various parameters in lengths of the hanging wall behind the support system at mechanized longwall (Oraee and Rostami, 2008). Quang et al. studied the behavior of the roof cave ability in different slopes by numerical modeling (Quang et al., 2008). Shabanimashcool et al., Behera et al., and Fei et al. studied the effect of mining activities on the failure and deformation characteristics of the strata using numerical modeling (Shabanimashcool et al., 2014; Behera et al., 2019; and Fei et al., 2020). Islavath et al. described a methodology for estimation of roof-to-floor convergence using 3D finite element models before and after web cut (Islavath et al., 2020). Noroozi et al. by using the theory of Peng (Peng, 1987), presented an analytical equation for calculating PRWEI (Noroozi et al., 2012). Also, Majdi et al. presented a mathematical-analytical model to calculate the height of the de-stress zone above the coal panel (Majdi et al., 2012). In addition, Hosseani et al. and Ansari Ardehjani et al. calculated and predicted the first and periodic roof weighting effect interval at the longwall panel using numerical modeling (Hosseini et al., 2014; Ansari Ardehjani et al., 2020). Hu et al. assessed the influence of stress on void ratios of compacted crushed rock masses in coal mine gobs (Hu et al., 2019). Darvishi et al. developed a numerical model to investigate the stability of a maingate, gate road named P8-maingate during caving and extraction of P7 and P8 coal panels of Tabas Parvadeh underground mine (Darvishi et al., 2020).

Bia et al. modeled the rock mass and support system using FLAC2D software and investigated the face spalling (Bai et al., 2014). Gao et al. used a new numerical approach to simulate progressive caving caused by extraction of a longwall mining panel (Gao et al., 2014). Wang et al. assessed the failure mechanism in the longwall method by using the UDEC software and found that more than 95% of the fractures are shear (Wang et al., 2016). Bai et al. analyzed the phenomenon of coal wall spall due to longwall mining based on experience and field observations (Bai et al., 2016). Using physical simulation and beam theory analysis, Li et al. found that the roof seam near the tailgate will fall by undercutting while the upper seam of the main gate moves slowly and never falls (Li et al., 2017). According to the literature, assessment of face stability and roof caving is very important in the longwall mining method, and there are only a few studies have been done on inclined coal seam in the longwall method.

Due to the Middle East tectonic conditions, coal seams in Iran are usually inclined, so the study of inclined seam behavior and face stability in different degrees in underground mining is necessary. In this paper, the face stability and behavior of gob roof seam in mechanized longwall mining are investigated by using numerical modeling. The modeling is validated based on Tabas Parvade coal mine geology and engineering data. For this purpose, four different block models have been simulated to assess the face and panel behavior in 0,5,10, and 15-degree slope in the FLAC3D software.

Case study

Tabas Parvadeh coal mine data was used for this research. The Tabas central coal mine (TCM) is the largest coal mine company in Iran located in the Tabas coal region, in the South Khorasan province, and it is the only fully mechanized longwall mine in the Middle East. This research has been done by simulating the E3 panel on different slopes. The E3 panel is located at a depth of 440 inside the coal seam C1. C1 coal seam in this panel has a slope of 20 degrees along its length and has a slope of 10 degrees along its width. Actually, the working face has a 20-degree slope in this panel. The thickness of the seam in this panel is brought in Table 1. It should be noted that coal extraction is made retreating along the seam C1 at the 10-degree slope (Tabas mines report).

Tab. 1. The thickness of E3 panel roof and floor seam (Tabas mines report (TPC), 2005)

Seam location	Type	Thickness (m)
Floor	Sandstone	6
Floor	Siltstone	3
Floor	Silty-Sandstone	5
E3 panel	Coal C1	2
Roof	Silty-Sandstone	16
Roof	Coal C2	1
Roof	Argillite	2
Roof	Silty-sandstone	18
Roof	Sandstone	7

Numerical modeling

To study the behavior of face and roof seam during the longwall mining, four-block models are constructed in FLAC3D software (Figure 1). To build models with different slopes, the model dimension in x and y coordinates are the same in all models, but the height is different. The value of roof displacement, face stress, and shear strain in gob roof, face, and roof above the face have been investigated in four block models. Rock mass properties, geological factors, and mining conditions are the same for all block models; only the seam slope is different. The Linear Mohr-Coulomb model is applied for the seam. The geomechanical properties for rock mass used for the block models are presented in Table 2.

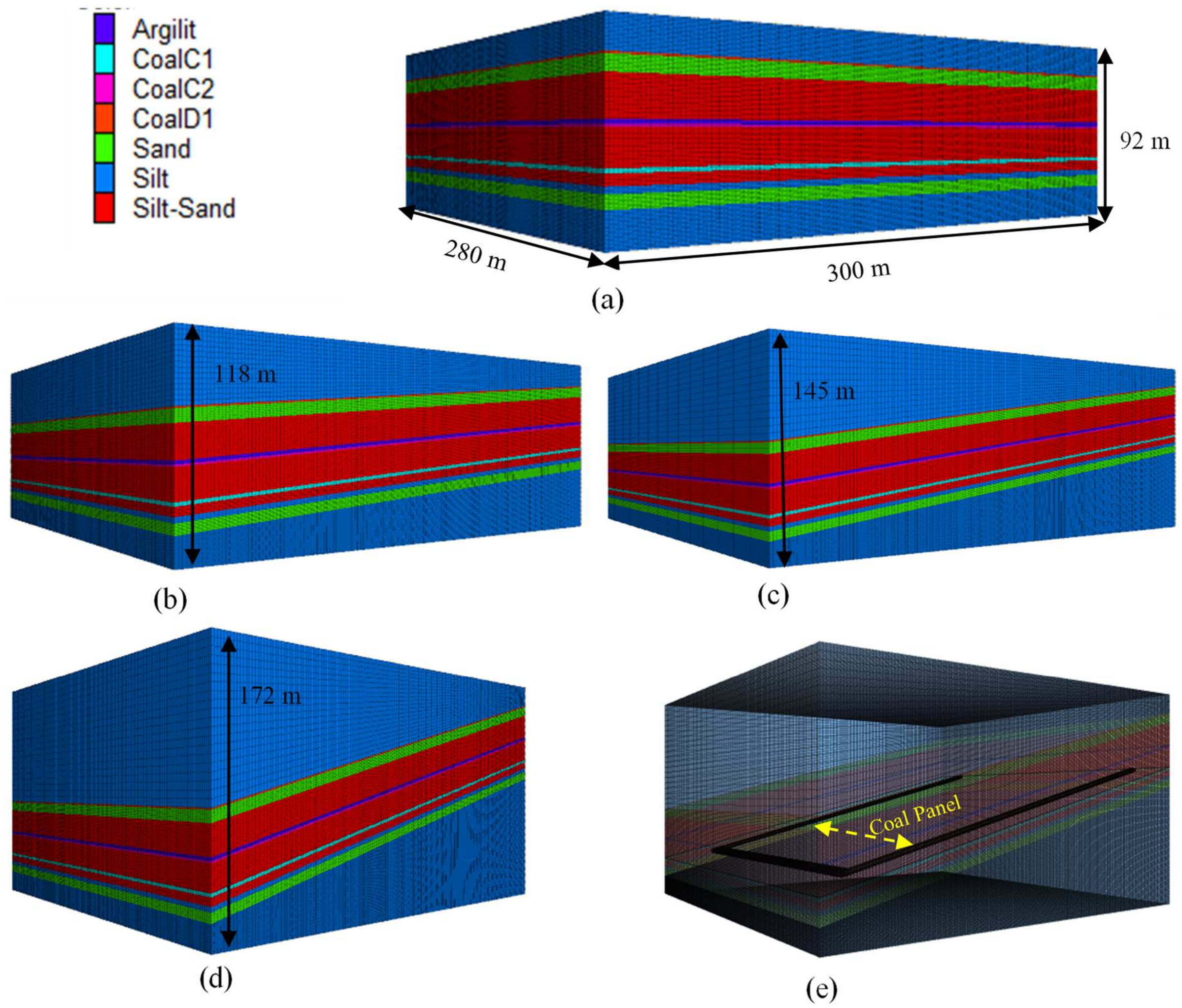

Fig. 1. (a): The model with zero-degree slope, (b): The model with 5-degree slope, (c): The model with 10-degree slope (d): The model with 15-degree slope (e): The coal panel opening in 15-degree slope

Tab. 2. Rock mass properties in E3 panel (Tabas mines report)

Rock type	Cohesion (MPa)	Friction angle (φ)	Tensile strength (MPa)	Poisson (ϑ)	Deformation modulus (GPa)	Dilation Angle
Siltstone	1.8	30	0.08	0.26	2.4	5
Silty-sandstone	4.26	50	0.09	0.25	2.34	5
Coal	0.33	34	0.009	0.25	0.09	2
Mudstone	0.18	26	0.017	0.31	1.86	5
Sandstone	4.25	35	0.1	0.25	2.72	5

After solving the constitutive model, the longwall openings were excavated when the model achieved the equilibrium, then support systems (rock bolts and steel frames) were installed. The sequence of drilling and opening diameter is similar to the main pattern of the Tabas Parvadeh coal mine. The main gate, Tail gate, and Bleeder widths, respectively, are 5 m, 5.5 m, and 7 m, and the height of those is 3 m. To reduce the model solving time, 350 m of the length of the openings were constructed in the model. An extensive load is applied on the working roof to model the powered support system. In addition to modeling the rock bolts and steel frames, the cable and beam elements in FLAC^{3D} are used, respectively.

After the development of the panels, the coal layer is extracted in 2-meter cuts until the first roof fall occurs. The values of roof displacement, face stress, and shear strain in gob roof, face, and roof above the face have been calculated in all block models. The flowchart of numerical modeling steps is shown in Figure 2. In this Figure, (Css) is the calculated shear strain in the numerical modeling and (Cri) is the critical amount of shear strain that is calculated by the Sakurai equation.

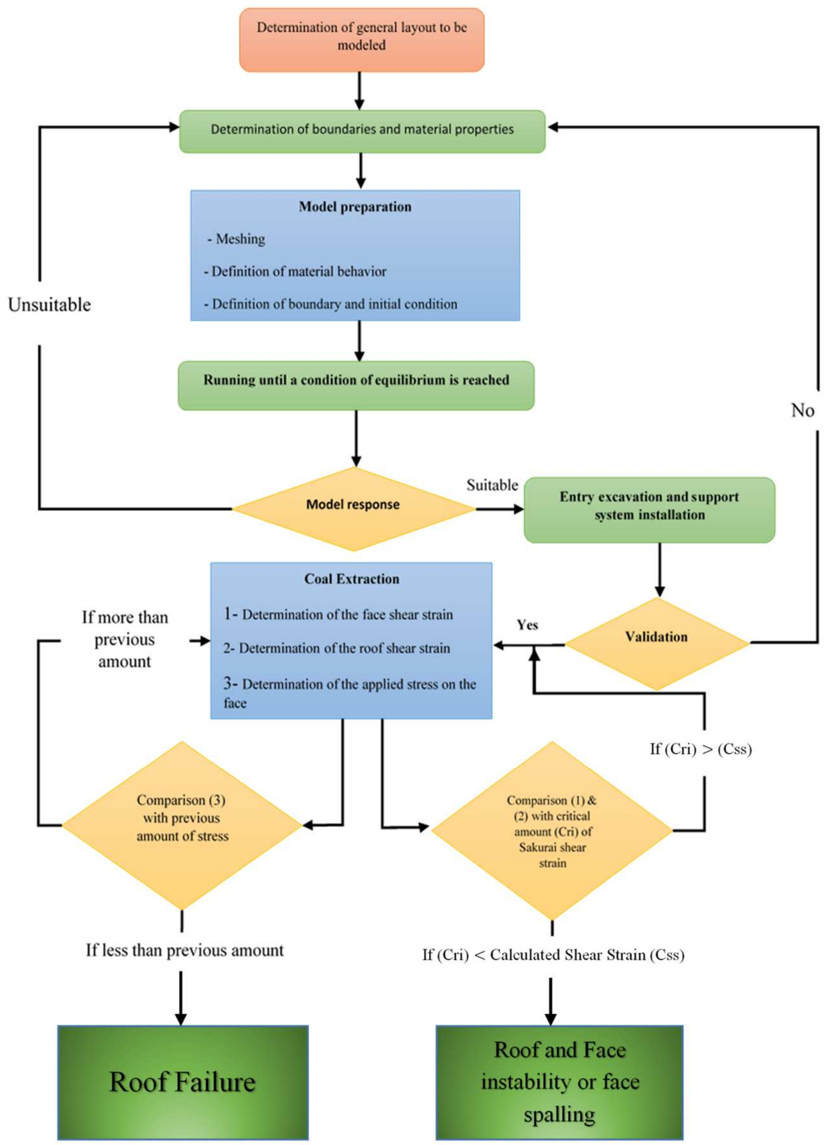

Fig. 2. Flowchart of numerical modeling steps for determining the roof failure and face stability

Validation

The vertical roof displacement data is extracted from the model before the coal extraction and compared with data extracted from the Telltale to validate the constructed model. The comparison graph of the extracted data from the Telltales and the data obtained from numerical modeling is shown in Figure (3b). According to this Figure, the results show a good agreement with the extracted data from the instrumentation and the numerical data. The location of history points in numerical modeling is shown in Figure (3c). The history points are placed exactly at the same place of Telltale in the gate road as Tabas mine.

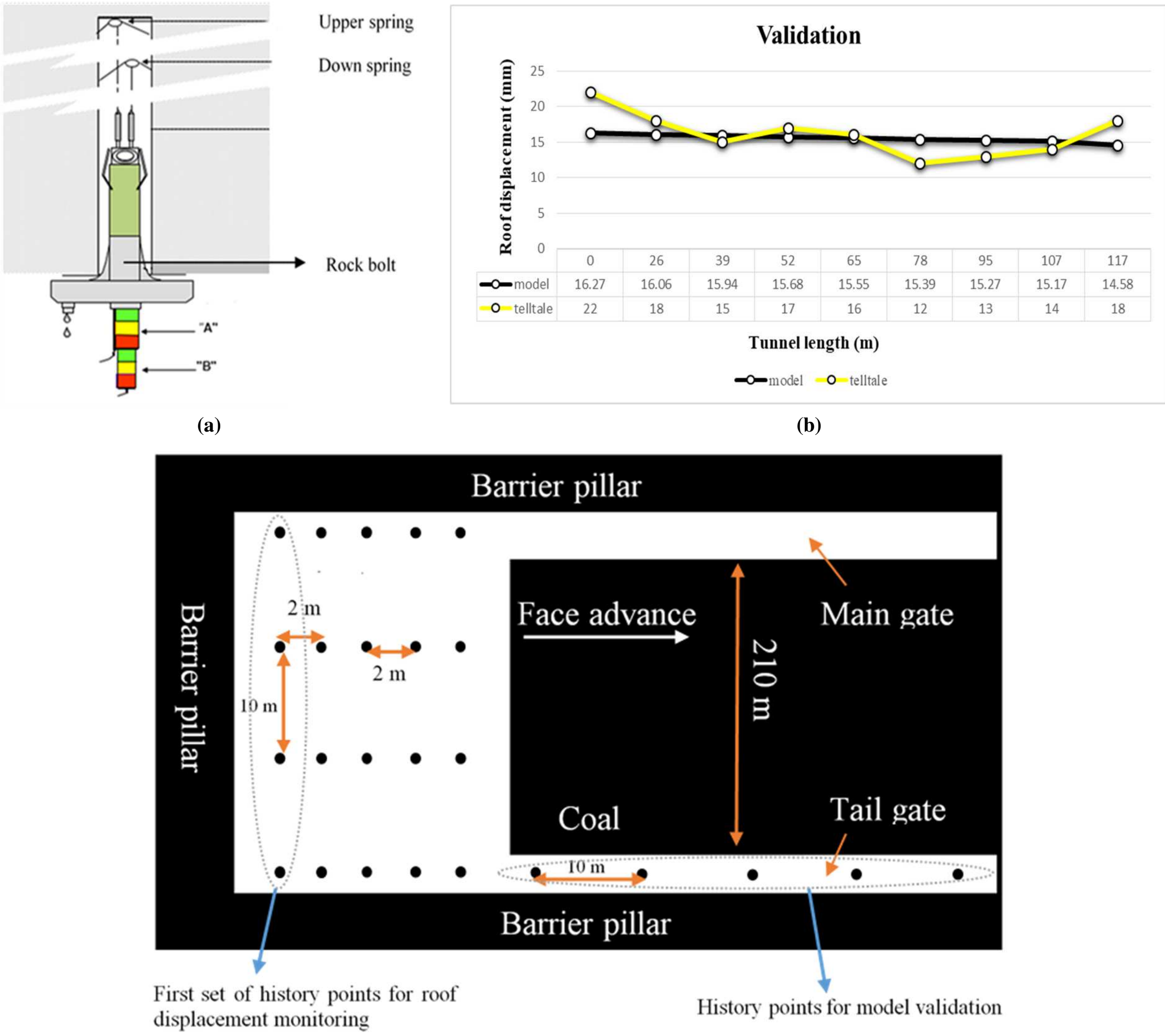

Fig. 3 a) The Telltale which is used in Tabas coal mine (Tabas mines report), b) Comparison between Telltale and numerical values c) The location of history points in the numerical modeling

Investigation behavior of the gob roof seam

Horizontal seam

Based on numerical modeling, by extracting the first coal cut in the horizontal seam, failure begins, and the shear cracks extension first occurs in the gob floor seam. In other words, the start of the failure in the gob begins with floor upward and failure extension in gob floor seam. By advancing the face and powered support, shear cracks gradually expand in the roof. Because of the installation of rock bolts near the barrier pillars, the roof failure starts developing from the top of the powered support system and the newly extracted area. But with the advance of the face, failure extends through the gob roof and floor.

In the horizontal seam, the height of the de-stressed zone in the roof and floor is, respectively, 8.5 and 3 times more than the extraction height. The height of the de-stressed zone in the gob roof and the floor are, respectively, 25 and 9 meters. After the first roof failure and stress drainage, all the model blocks with shear conditions reached the equilibrium state. The shear stress started again from the first roof failure position and gradually entered the de-stressed zone by continuing coal extraction. The expansion of the roof and floor seam failure process duo to coal extraction from the first coal cut to the twelfth cut is shown in Figure 4.

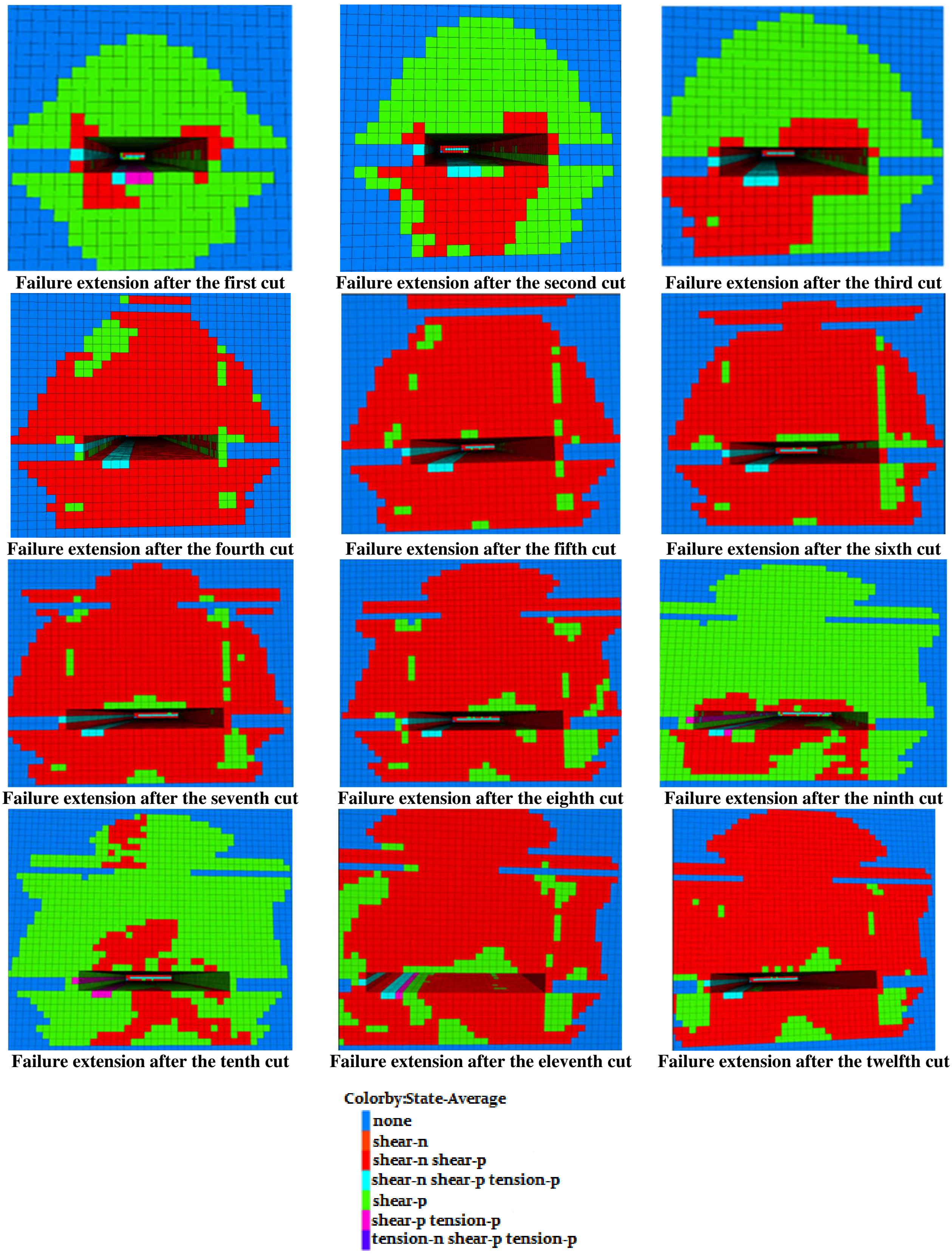

Fig. 4. Failure extension from the First cut to the 12th cut

Figure 4 shows that after the 9th cut extraction, stress discharges and failure occurred in the rock mass because, after this cut extraction, the blocks have been reached from shear to post-shear condition. With continuing coal extraction, the blocks in the middle span of gob from stable condition gradually reach shear condition. By studying the vertical stress changes in each cut and drawing the face vertical stress diagram, it concluded that after the ninth cut extraction, the vertical stress curve changes a descending trend, and the concentration of stress on the face is reduced. So, the first roof failure time is after the ninth cut extraction, and the value of FRWEI is calculated as 26 meters. The face vertical stress changes before and after the failure are shown in Figure 5. According to these figures, the concentration of stress occurs approximately 7 to 8 meters from the face and barrier pillar. The graph of changes in vertical stress after each coal cut is shown in Figure 6.

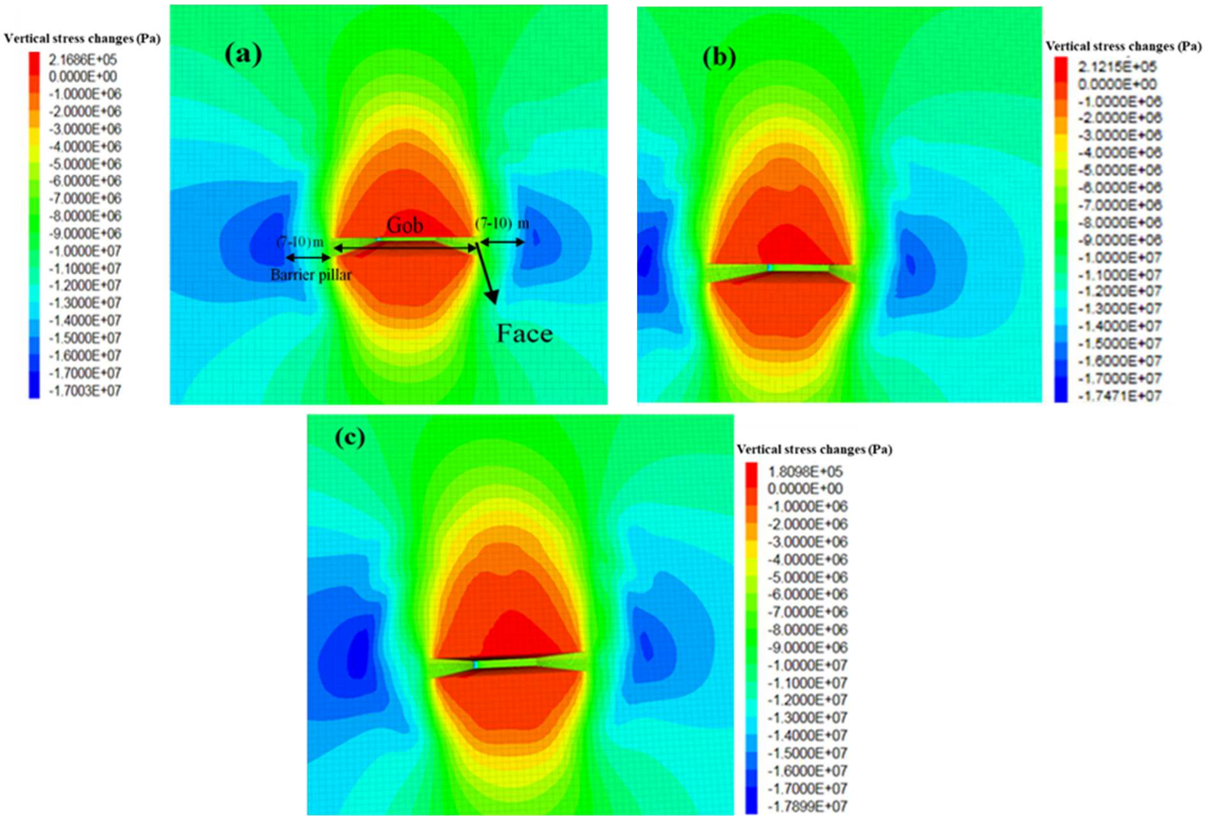

Fig. 5. The contour of vertical stress in the seventh, eighth and, the ninth cut (respectively a, b and c)

Fig. 6. The Vertical stress variation diagram on the face for each coal cut extraction in a horizontal seam

The diagram of the average displacement of the caving zone before and after failure for stress variations in each coal cut extraction is shown in Figure 7. According to this chart, roof displacement is increased by extracting each coal cut. But in the ninth cut, the rising trend of displacement value is stopped, and roof displacement is decreased. By examining this chart, reducing displacement values is due to the reduction of the applied stress on the roof and face and roof failure, which is occurred in this cut.

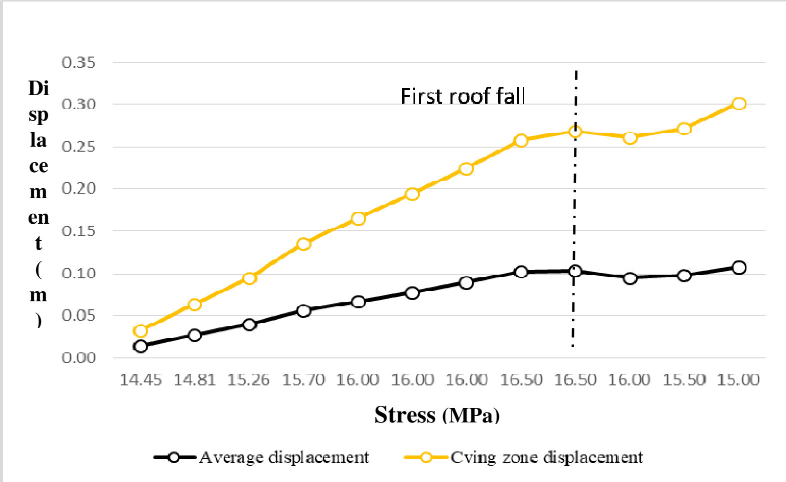

Fig. 7. The value of average and total caving zone displacement related to the stress in each cut

Inclined seam

In the next step, three other models with slopes of 5, 10, and 15 degrees are constructed. Different stress graphs are obtained by modeling the extraction panel with different slopes (Figures 8). Based on these graphs, after coal extraction and face advance, the applied stress on the face is increased, but when the stress value is between 16 to 17 MPa, the upward trend of the stress graph is stopped and declined. In other words, all of these graphs at the failure time show a 16 to 17 MPa stress value. Also, roof failure at 5, 10, and 15-degree slope, respectively, occurs at the cut number 10, 11, and 14. The FRWEI value for 5, 10, and 15-degree slopes is calculated as 29.09, 31.38, and 36 meters. By comparing the trend of stress variation on different slopes, it can be concluded that with increasing seam' slope, the time to reach the failure, stress is increased. In other words, for roof failure and stress discharge, more coal cutting numbers should be extracted. This means that with increasing the layer's slope, the FRWEI value will increase. The first roof weighting effect interval on each slope and the cut number associated with the time of roof failure is shown in Figure 9.

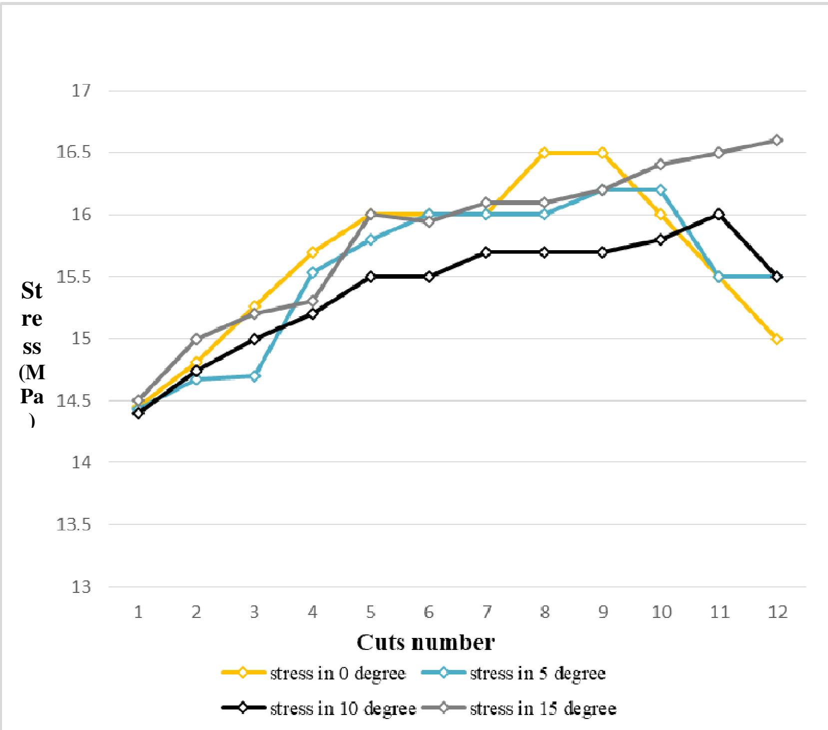

Fig. 8. Comparison of stress variations in different slopes for 12 coal cut extraction

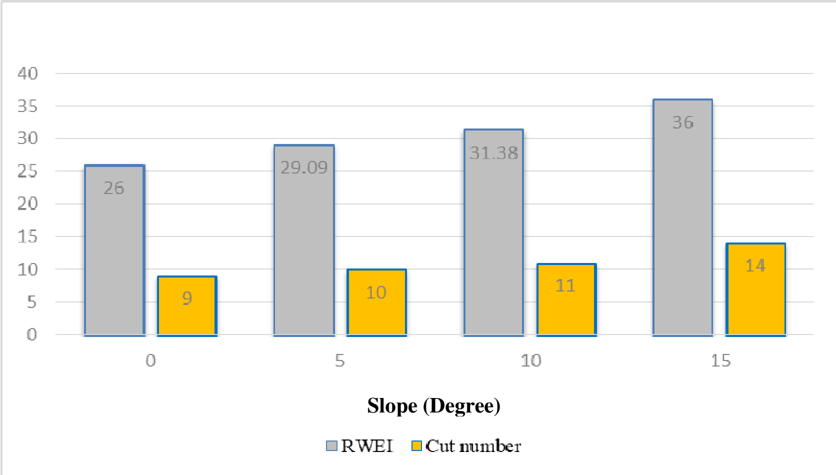

Fig. 9. FRWEI value for each slope and the cut number associated with the time of roof failure

By excavating an underground space, the seam that is on top of this space moves toward the empty space and bends. So, the unsupported roof falls under its weight. Accordingly, due to coal extraction in the longwall mining, the vertical displacement of the roof gradually increases. The vertical roof displacement depends on a few factors including, the layer's thickness, joint conditions, dimensions of the gob, the layer's slope, etc. Based on numerical modeling results, vertical roof displacement will be reduced after the coal extraction by increasing the layer's slope. That happens because the increased slope causes the weight of the layer to be decomposed along with it and will add an additional load to the seam head. Due to this additional load and its reaction force, the horizontal in-situ stress will increase along with the layer. Increasing horizontal in-situ stress (in a certain range) causes the blocks created by the extension of shear joints to be latched and will increase the resistance of the seam. On the other hand, in the slope seam, only a part of the gravity force affects the layer, which is equal to $w \times sin\alpha$ (w is the layer weight and α is the layer slope). The other part of gravity force ($w\ cos\alpha$) increases the horizontal in situ stress on the seam head. This compressive force increases the friction and cohesion along the shear joints and reduces the impact of tensile weight force. So, the vertical roof displacement and the RWEI value will increase by increasing the slope. Figures 10 and 11 show that the vertical roof displacement is compared with other displacement values on different slopes.

In the horizontal seam, due to the sudden decrease of stress on the roof and the face following the First Roof Weighting Effect, the vertical roof displacement is decreased relative to slope conditions. However, by assessing the diagram of roof total displacement in different slopes (Figure 10), before the roof failure in the horizontal seam (before the 9th cut extraction), roof displacement in the horizontal seam is larger than the slope condition of seams (Figure 11). As a result, this displacement decreased due to the reduction of applied stress on the roof and face.

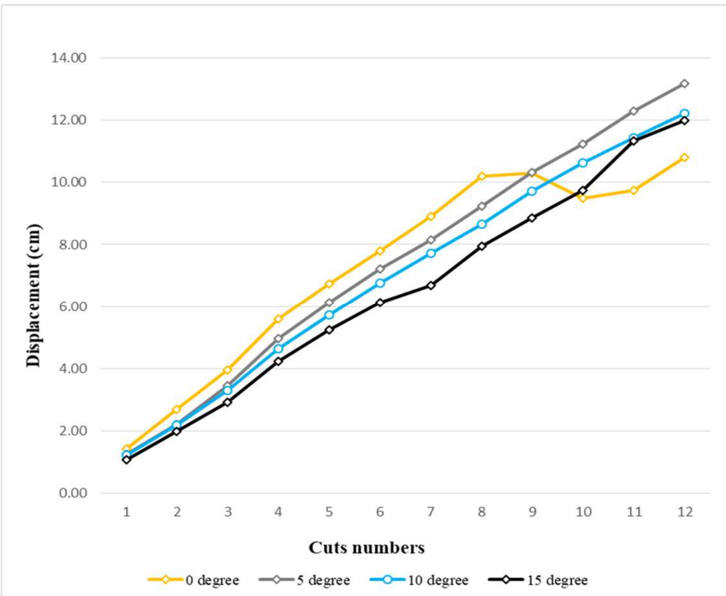

Fig. 10. Comparison of average roof displacement in different slopes following 12 coal cut extraction

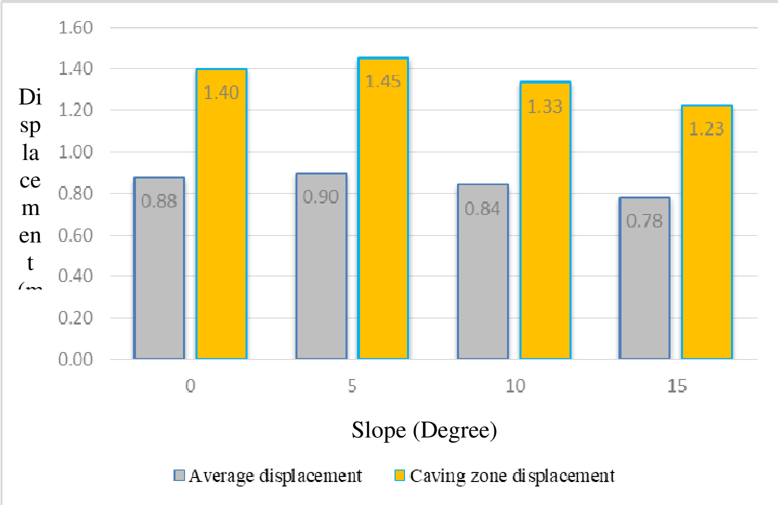

Fig. 11. Comparison of average roof displacement and caving zone in different slopes following 12 coal cut extraction

Therefore, by increasing the seam slope in a certain range, layer resistance, vertical layer displacement, and subsequently, surface subsidence will decrease, and the hanging wall failure ability will decrease. So, to design a caving space in the sloping seam, other parameters such as undercut dimensions, apply loads, and roof cave by blasting should also be considered.

Influence of slope increasing on the face stability

Another important issue in longwall mining is the face stability and reduction of the effect of gob stress on the face and face spalling during coal extraction. In this case, due to the stress concentration in the intersection between the roof, and the face, shear joints are created, and blocks are formed in this area. These created blocks may fall before coal extraction. By increasing the Tip-to-Face distance (the distance between the face and the powered support system), the value of face stress increases, which will raise the risk of coal fall. This study's roof and face materials are silty sandstone and coal.

To study the strata's behavior, the Sakurai criterion, which is developed to investigate the underground space's stability, has been used. To this aim, the strata shear strain values, which are calculated from numerical modeling, are compared with the critical shear strain calculated in the Sakurai equations. The critical shear strain of strata is calculated by using Equations 1 and 2 (Sakurai, 1997). The calculated values of the critical shear strain by using the Sakurai equations are presented in Table 3. If the value of the calculated shear strain in numerical modeling is greater than the critical shear strain, the strata are unstable, and probably the failure has happened.

$$\log\varepsilon_c = -0.25\log E - 1.22 \quad (1)$$

$$\gamma_C = (1+\vartheta)\times\varepsilon_c \quad (2)$$

Tab. 3. The calculated value of critical shear strain by Sakurai Equation

Rock type	Poison's ratio (ϑ)	E module (GPa)	Critical strain $\varepsilon_c \times 10^{-3}$	Critical shear strain $\gamma_C \times 10^{-3}$
Silty sandstone	0.26	2.4	4.82	6.07
coal	0.25	0.09	10.94	13.68
Sandstone	0.25	2.72	5.83	5.83

Based on numerical modeling results, after extraction of the first and second coal cut in a horizontal seam, the face and roof are stable. But, by extraction of the third coal cut, the shear strain value of face and roof is equal to a critical amount of shear strain, which is calculated in the Sakurai Equations. In this case, the face and roof will be on the verge of collapse. By extracting the fourth coal cut, the shear strain is more than the critical value in the face and roof, which causes failure and instability. As face advance continues, the roof and face are unstable until the first roof fall in the ninth section occurs. The face and roof shear strain change process after 12 coal cut extraction are shown respectively in Figures 12 and 13.

In the next step, the panel was modeled in the seam with 5-, 10- and 15-degree slopes, then coal was extracted. According to Figure 12, the face shear strain in the seam with a 5-degree slope before the eighth cut extraction is close to the critical value. In other words, from the first time of the coal cut until extracting the seventh cut, the face may be broken. But after extraction of the eighth cut, the face shear strain is increased. This uptrend continues only after the ninth coal cut extraction, and with the extraction of the tenth cut, this value is decreased with the first roof failure. After the tenth cut extraction, the face shear strain is less than the critical value and stable. Generally, it can be said that the calculated strain in the seam with a 5-degree slope is lower than that of in horizontal seam, and the face experiences less pressure. The roof top of the face in a 5-degree slope seam is more unstable than the face in this condition. The roof is also stable after the first roof fall in the tenth cut extraction. So, less stress on the roof and face in a 5-degrees slope relative to the horizontal seam is applied.

The face shear strain variations in the seam with 0-, 5-, 10- and 15-degree slopes are shown in Figure 12. In this Figure, when the seam slope increases, the face stability increases. In other words, when the slop of seam increases, the value of face shear strain reduces, and only in the first time of roof fall, the face is unstable. As a result of increasing the slope, the time to achieve face instability increases, and the severity of instability decreases. Therefore, by increasing the slope seam, less cost and time will be spent for the roof supporting and face stability. As the slope increases, the roof stability condition is similar to the face stability condition. The roof shear strain variations in the seam with 0, 5, 10, and 15 degrees of a slope are shown in Figure 13. The change process of roof instability is similar to the face in the horizontal seam, and after two coal cut extractions, the roof is unstable. This instability continues until the first roof fall has occurred. Based on numerical modeling, by increasing the slope, roof instability reduces. On the slope of 15 degrees in two cuts, before the first roof fall occurs, the roof is unstable, and on a 10-degree slope after extraction of the 8th cut, the roof is unstable. While in a 5-degree slope, this phenomenon has occurred after the third coal cut extraction.

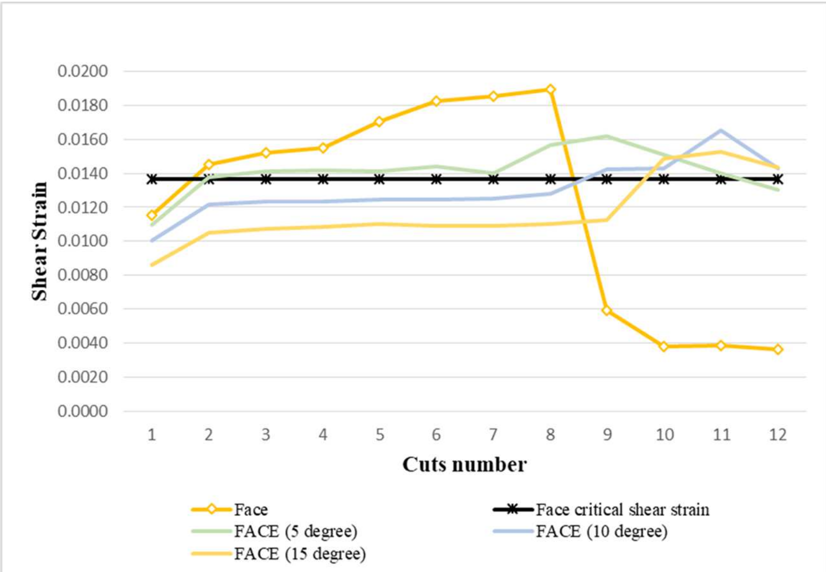

Fig. 12. The face shear strain variations in the seam with 0, 5, 10, and 15 degrees of slope

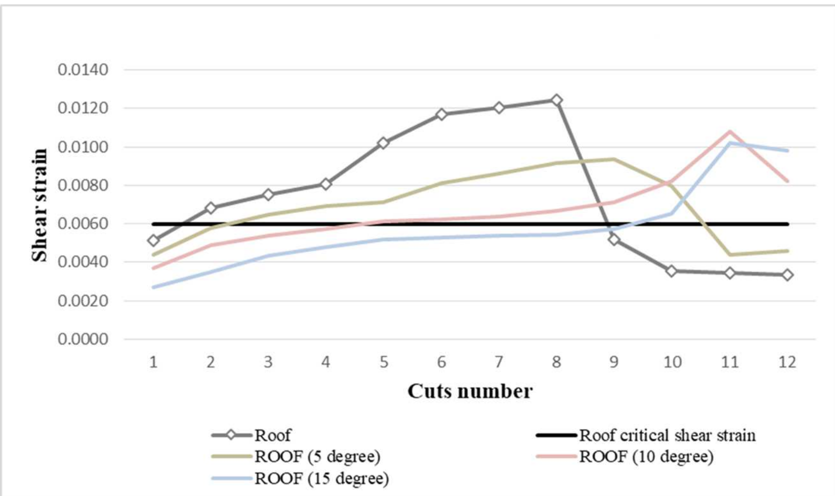

Fig. 13. The roof shear strain variations in the seam with 0, 5, 10, and 15 degrees of slope

Discussion

Several factors affect the time of roof failure and face stability. However, due to the specific geological conditions in Iran, limited coal resources, and the need to develop safety in the mines, the slope has been studied as an influential factor in the roof and face behavior. The changes in this parameter affect the production, safety, and economic mining operation.

The time to apply the maximum stress that is required for layer failure will go up with an increase in the layer slope. Thus the vertical layer displacement decreases, and the FRWEI value increases. It will happen when stress applied on the seam at the time of failure is within the same range, and all the seams in different slopes are broken in the stress range of 16-16.5 MPa for the first time. In order to have a roof fall, the stress must be within the range of 16-16.5 MPa; by increasing the seam slope, the time required to reach this range is increased. This time increase is only due to the increased horizontal in-situ stress and the layer weight force decomposition. In other words, by increasing the seam slope, the stability time increases, and in order to have a roof failure in these conditions, dimensions of the drilling space should be increased. When the seam is horizontal, the face and its upper roof before the first roof fall are always prone to collapse. However, by increasing the slope, only in the last two extraction cuts before the first roof fall in the gob, the face and roof are prone to fall. After the first roof failure, the face and roof are stable, and there is no need for maintenance and consolidation.

Conclusions

The coal seams in Iran are generally steep due to the special tectonic conditions in the Middle East. Therefore, it is necessary to study the behavior of the inclined seam and face stability in different degrees of a slope. Thus, this work investigates the face stability and behavior of the gob roof seam in a mechanized longwall method using numerical modeling. The modeling was validated using the Tabas Parvade coal mine geology and engineering data. For this purpose, four different models were simulated to assess the face and panel roof behavior in the 0-, 5-, 10-, and 15-degrees of a slope using the FLAC3D software. These models were validated based on the simulation of the E3 panel in the Tabas Parvade coal mine.

Based on the numerical modeling results, the values of FRWEI in the 0-, 5-, 10-, and 15-degree slopes were calculated to be equal to 26, 29.09, 31.38, and 36 m, respectively. By comparing the trend of stress variation in different slopes, it can be concluded that the time to reach the breaking point increases by increasing the layer slope. In order to have a roof failure and stress discharge, further cuts should be extracted. This means that when the seam slope increases, the FRWEI value will increase. In a horizontal seam, the face and roof top of the face before the first roof fall are prone to fall. However, by increasing the seam slope, only in the last two cuts before the first roof fall in the gob, the face and roof are prone to fall. After the first roof failure, the face and roof are stable and do not require any support. In other words, by increasing the layer slope, the face stability and its upper roof are improved.

For a good longwall mining method, many factors are effective. According to this research work, the stress applied to the barrier pillar and coal face increases due to the slope increase. Thus, investigating the effect of seam slope on the barrier and chain pillar size and strength in the longwall mining is recommended.

References

Ardehjani, E. A., Ataei, M. and Rafiee, R. (2020). Estimation of first and periodic roof weighting effect interval in mechanized longwall mining using numerical modeling. *International Journal of Geomechanics*, *20*(2), 04019164.

Ataei, M. (2015). Underground caving method, Shahrood, Iran, *Shahrood University of Technology*.

Bai, Q.S., Tu, S.H., Zhang, C. and Zhu, D. (2016). Discrete element modeling of progressive failure in a wide coal roadway from water-rich roofs. *International Journal of Coal Geology, 167, pp.215-229*.

Bai, Q.S., Tu, S.H., Zhang, X.G., Zhang, C. and Yuan, Y. (2014). Numerical modeling on brittle failure of coal wall in longwall face—a case study. *Arabian Journal of Geosciences, 7(12), pp.5067-5080.*

Behera, B., Yadav, A., Singh, G.S.P. and Sharma, S.K. (2020). Numerical modeling study of the geo-mechanical response of strata in longwall operations with particular reference to Indian geo-mining conditions. *Rock Mechanics and Rock Engineering, 53(4), pp.1827-1856.*

Chen, J., Zhou, L., Xia, B., Su, X. and Shen, Z. (2021). Numerical investigation of 3D distribution of mining-induced fractures in response to longwall mining. *Natural Resources Research, 30(1), 889-916*.

Darvishi, A., Ataei, M. and Rafiee, R. (2020). Investigating the effect of simultaneous extraction of two longwall panels on a maingate gateroad stability using numerical modeling. *International Journal of Rock Mechanics and Mining Sciences, 126, 104172*.

Das, S. K. (2000). Observations and classification of roof strata behaviour over longwall coal mining panels in India. *International Journal of Rock Mechanics and Mining Sciences, 37(4), 585-597.*

Fei, Y., Liu, S., Xu, Y. and Zhao, L. (2020). Failure Analysis of Thin Bedrock and Clay Roof in Underground Coal Mining: Case Study in Longdong Coal Mine. *International Journal of Geomechanics, 20(10), 04020187.*

Gao, F., Stead, D. and Coggan, J. (2014). Evaluation of coal longwall caving characteristics using an innovative UDEC Trigon approach. *Computers and Geotechnics, 55, 448-460.*

Hu, S., Han, D., Feng, G., Zhang, A., Hao, G., Hu, L. and Li, B. (2020). Influence of stress on void ratios of compacted crushed rock masses in coal mine gobs. *Natural Resources Research, 29(2), 1361-1373.*

Itasca, FLAC-3D (Version 5.0) user manual, ed: Itasca Cons Group Inc Minneapolis, MN, (2012).

Islavath, S.R., Deb, D. and Kumar, H. (2020). Development of a roof-to-floor convergence index for longwall face using combined finite element modelling and statistical approach. *International Journal of Rock Mechanics and Mining Sciences, 127, 104221.*

Li, X., Wang, Z. and Zhang, J. (2017). Stability of roof structure and its control in steeply inclined coal seams. *International Journal of Mining Science and Technology, 27(2), 359-364.*

Majdi, A., Hassani, F.P. and Nasiri, M.Y. (2012). Prediction of the height of de-stressed zone above the mined panel roof in longwall coal mining. *International Journal of Coal Geology, 98, 62-72.*

Noroozi, A., Oraee, K., Javadi, M., Goshtasbi, K. and Khodadady, H. (2012). A model for determining the breaking characteristics of immediate roof in longwall mines. *Yerbilimleri, 33(2), 193-203.*

TPC (Tabas Parvadeh Coal). 2005. Basic design of Tabas coal mineproject. *Tabas, South: TPC.*

Oraee, K. and Rostami, M. (2008). Qualitative and quantitative analysis of hangingwall caving in longwall mining method using a fuzzy system. *In 21st world mining congress & expo.*

PENG, S.S. 1987. Longwall automation grows. Coal Min. *Process.;(United States), 24.*

Quang, D.H., Cai, Y. and Hebblewhite, B. (2008). Numerical analysis of some Geotechnical factors influencing the application of Longwall Top Coal Caving. *In The 27th International Conference on Ground Control in Mining (pp. 222-228).*

Sakurai, S. (1997). Lessons learned from field measurements in tunnelling. *Tunnelling and underground space technology, 12(4), 453-460.*

Shabanimashcool, M., Jing, L. and Li, C.C. (2014). Discontinuous modelling of stratum cave-in in a longwall coal mine in the arctic area. *Geotechnical and Geological Engineering, 32(5), 1239-1252.*

Wang, J., Yang, S. and Kong, D. (2016). Failure mechanism and control technology of longwall coalface in large-cutting-height mining method. *International Journal of Mining Science and Technology, 26(1), 111-118.*